Bayesian Approach with Maximum Entropy Priors to Imaging Inverse Problems. Part II : Applications *

Ali Mohammad–Djafari
Laboratoire des Signaux et Systèmes (CNRS–ESE–UPS)
École Supérieure d'Électricité
Plateau de Moulon, 91192 Gif–sur–Yvette Cedex, France.

Abstract

This paper is the second of two papers on Bayesian approach with maximum entropy priors to imaging inverse problems. In the first part we proposed a method based on the Maximum a posteriori (MAP) Bayesian approach with Maximum Entropy (ME) priors to solve the linear system of equations which is obtained after the discretisation of the integral equations which arise in various tomographic image restoration and reconstruction problems. In this second part we present some of the imaging applications in which we used the proposed method. These applications are image restoration, microwave tomographic image reconstruction and a new tomographic imaging approach to Eddy current non destructive control of conducting media.

*submitted to *IEEE Trans. on Image Processing*, August 1993. rejected on 1995.

1 Introduction

In the first part [**?**] we addressed a class of image reconstruction and restoration problems which is to solve the integral equations of the form:

$$g_{ij} = \int_D f(\boldsymbol{r}')\, h_{ij}(\boldsymbol{r}')\, \mathrm{d}\boldsymbol{r}' + b_{ij}, \quad i,j = 1,\cdots,M, \tag{1}$$

where $\boldsymbol{r}' \in \mathbb{R}^2$, $f(\boldsymbol{r}')$ is the object (image reconstruction problems) or the original image (image restoration problems), g_{ij} are the measured data (the projections in image reconstruction or the degraded image in image restoration problems), b_{ij} are the measurement noise and $h_{ij}(\boldsymbol{r}')$ are known functions which depend only on the measurement system. To show the generality of this relation, we give in the following some of the applications that we are interested in :

- 1–D signal deconvolution :

$$g(t_i) = \int_0^t f(t')\, h(t_i - t')\, \mathrm{d}t' + b(t_i), \quad i = 1,\cdots,M, \tag{2}$$

  where $g(t_i)$ are the degraded signal samples and $h(t)$ is the impulse response of the measurement system.

- X–ray radiography of cylindrical symmetric objects :

$$g(r_i) = \int_{r_i}^R f(\rho)\, \frac{\rho}{\sqrt{\rho^2 - r_i^2}}\, \mathrm{d}\rho + b(r_i), \quad i = 1,\cdots,M \tag{3}$$

  where $g(r_i)$ is the measured intensity of the film darkeninig, $f(\rho)$ is the radial X–ray optical density profile, r_i are the radial distances of the measurement points and R is the radius of the object. We can remark that this integral is the Abel transform integral which is encountered in many other physical experiments such as Plasma physics.

- Image restoration :

$$g(x_i,y_j) = \iint_D f(x',y')\, h(x_i - x', y_j - y')\, \mathrm{d}x'\, \mathrm{d}y' + b(x_i,y_j), \qquad \begin{matrix} i = 1,\cdots,N \\ j = 1,\cdots,M \end{matrix}, \tag{4}$$

  where $g(x_i,y_j)$ are the observed degraded image pixels and $h(x,y)$ is the point spread function (PSF) of the measurement system.

- X–ray computed tomography (CT) :

$$g(r_i,\phi_j) = \iint_D f(x,y)\, \delta(r_i - x\cos\phi_i - y\sin\phi_i)\, \mathrm{d}x\, \mathrm{d}y + b(r_i,\phi_j), \qquad \begin{matrix} i = 1,\cdots,N \\ j = 1,\cdots,M \end{matrix}, \tag{5}$$

  where $g(r_i,\phi_j)$ are the projections along the axis $r_i = x\cos\phi_i - y\sin\phi_i$, having the angle ϕ_j, and which can be considered as the samples of the Radon transform (RT) of the object function $f(x,y)$.

- Fourier Synthesis in radio astronomy or in SAR imaging systems :

$$g(u_j,v_j) = \iint_D f(x,y)\, \exp\left[-j(u_j x + v_j y)\right]\, \mathrm{d}x\, \mathrm{d}y + b(u_j,v_j), \quad j = 1,\cdots,M \tag{6}$$

  where $\boldsymbol{u}_j = (u_j,v_j)$ is a radial direction and $g(u_j,v_j)$ are the samples of the complex valued visibility function of the sky in radio astronomy or the Fourier transform of the measured signal in SAR imaging.

- Fourier Synthesis in X–ray CT, nuclear magnetic resonance (NMR) imaging or diffraction tomography [1, 2, 3] :

$$g(\Omega_i, \phi_j) = \iint_D f(x,y)\, \exp\left[-j\,(T_1(\Omega,\phi_j)x + T_2(\Omega,\phi_j)y)\right]\, \mathrm{d}x\, \mathrm{d}y, \qquad \begin{matrix} i = 1, \cdots, N \\ j = 1, \cdots, M \end{matrix}\ , \tag{7}$$

where

$$\left\{ \begin{array}{rcl} u & = & T_1(\Omega,\phi) \\ v & = & T_2(\Omega,\phi) \end{array} \right. \tag{8}$$

define a finite set of algebraic contours in the Fourier domain (u,v) of the object. This general FS formulation is interesting, because it is in the heart of many imaging systems:

  - In X–ray CT and in NMR imaging we have :

$$\begin{pmatrix} u = T_1(\Omega,\phi) \\ v = T_2(\Omega,\phi) \end{pmatrix} = \begin{pmatrix} \cos\phi & \sin\phi \\ -\sin\phi & \cos\phi \end{pmatrix} \begin{pmatrix} \Omega \\ 0 \end{pmatrix} \tag{9}$$

    where the algebraic contours are the concentric straight lines. In X–ray CT $g(\Omega_i, \phi_j)$ are related to the discrete Fourier transform (DFT) of the projections $p(r_i, \phi_j)$, while, in NMR imaging $g(t_i, \phi_j)$ are directly the samples of free precession NMR signals.

  - In diffraction (ultrasound or microwave) tomography we have:

$$\begin{pmatrix} u = T_1(\Omega,\phi) \\ v = T_2(\Omega,\phi) \end{pmatrix} = \begin{pmatrix} \cos\phi & \sin\phi \\ -\sin\phi & \cos\phi \end{pmatrix} \begin{pmatrix} -k_0 + \sqrt{k_0^2 - \Omega^2} \\ \Omega \end{pmatrix}, \tag{10}$$

    where k_0 is the propagation constant of the medium surrounding the object, $f(x,y)$ is either the contrast function of the ultrasound velocity or the contrast function of the complex permittivity of object. The algebraic contours in this case are the concentric semi-circles.

- Fourier–Laplace synthesis arising in nondestructive Eddy current tomographic imaging :

$$g(u_i, s_j) = \iint_D f(x,y)\, \exp\left[j\,(u_i x + s_j y)\right]\, \mathrm{d}x\, \mathrm{d}y + b(u_i, s_j), \qquad \begin{matrix} i = 1, \cdots, N \\ j = 1, \cdots, M \end{matrix}\ , \tag{11}$$

where $f(x,y)$ is the contrast function of the conductivity in the object, u is the spatial frequency horizontal axis and $s = \gamma + jv$ is a complex value with γ representing the attenuation and v the propagation. (u,v) is also a point in the spatial Fourier domain of the object $f(x,y)$ and $g(u_i, s_j)$ are related to the Fourier Transform of the measured diffracted field [4, 5].

In all these applications we have to solve the following ill-posed problem: estimate a function $f(x,y)$ from some finite set of measured data which may also be noisy, because there is no experimental measurement device, even the most elaborate, which could be entirely free from uncertainty, the simplest example being the finite precision of the measurements.

In many of these image reconstruction and restoration problems $f(x,y)$ represents the spatial distribution of a positive quantity (for example the conductivity or the density of the matter inside the examined object). So, when discretised these problems can be described by the following discrete problem:

> Estimate a positive vector $\boldsymbol{x} \in \mathbb{R}_+^n$ (representing the pixel intensities in an image) given a vector of measurements $\boldsymbol{y} \in \mathbb{R}^m$ (representing, for example, either a degraded image pixel values in restoration problems or the projections values in reconstruction problems) and a linear transformation $\boldsymbol{A}$ relating them by:

$$\boldsymbol{y} = \boldsymbol{A}\boldsymbol{x} + \boldsymbol{b}, \tag{12}$$

where $\boldsymbol{b}$ represents the discretisation errors and the measurement noise which is supposed to be zero-mean and additive.

In the first part of this paper [?] we proposed a method based on the Bayesian approach with maximum entropy priors to find a regularised solution to this problem.

2 Outline of the proposed method

What we proposed in the first part of this paper was to use the Bayesian framework and the ME principle to solve inverse problems arising in image reconstruction and restoration applications. We discussed first in detail how to assign a prior law $p(\boldsymbol{x})$ which only reflects our prior knowledge about the image. We showed that, with some global constraints on the image $\boldsymbol{x}$,*i.e.*; knowing that $x_j > 0$ and two statistical constraints which are the expectation of two functions $\phi_1(\boldsymbol{x})$ and $\phi_2(\boldsymbol{x})$, $p(\boldsymbol{x})$ is in the form:

$$p(\boldsymbol{x}) \propto \exp\left[-\lambda\phi_2(\boldsymbol{x}) - \mu\phi_1(\boldsymbol{x})\right] \quad \text{with} \quad \phi_2(\boldsymbol{x}) = \sum_{j=1}^{n} H(x_j) \quad \text{and} \quad \phi_1(\boldsymbol{x}) = \sum_{j=1}^{n} S(x_j) \tag{13}$$

We discussed then about the possible forms of the functions S and H which insures a scale invariance property and showed that (S, H) can be one of the following:

$$\Big\{S(x), H(x)\Big\} = \Big\{(x^{r_1}, x^{r_2}), (x^{r_1}, \ln x), (x^{r_1}, x^{r_1}\ln x), (\ln x, \ln^2 x)\Big\}. \tag{14}$$

We considered then the case where $S(x) = x$, and so where $H(x)$ is one of the following:

$$\Big\{H(x)\Big\} = \Big\{x^r, \ln x, x\ln x\Big\}. \tag{15}$$

Assuming then that what we know about the noise $\boldsymbol{b}$ is its covariance matrix $\boldsymbol{R}_b = \sigma_b^2\boldsymbol{I}$ and using the ME principle we showed that

$$p(\boldsymbol{y}|\boldsymbol{x}) \propto \exp\left[-Q(\boldsymbol{x})\right], \quad \text{with} \quad Q(\boldsymbol{x}) = \frac{1}{2}(\boldsymbol{y} - \boldsymbol{A}\boldsymbol{x})^t\boldsymbol{R}_b^{-1}(\boldsymbol{y} - \boldsymbol{A}\boldsymbol{x}), \tag{16}$$

and, finally, using the Bayes' rule to calculate the posterior law $p(\boldsymbol{x}|\boldsymbol{y})$ and MAP estimation, the solution is obtained by :

$$\widehat{\boldsymbol{x}} = \arg\min_{\boldsymbol{x}>0}\left\{J(\boldsymbol{x};\lambda,\mu) = Q(\boldsymbol{x}) + \lambda\phi_2(\boldsymbol{x}) + \mu\phi_1(\boldsymbol{x})\right\} \tag{17}$$

which can also be considered as the solution of a regularisation problem in which (λ, μ) are the regularisation parameters (hyperparameters). Then we addressed the two main difficulties in real applications which are:

- How to optimise the criterion (17) when the hyperparameters (λ, μ) are fixed ?
- How to determine the hyperparameter values (λ, μ) from the available data $\boldsymbol{y}$?

For the first, we propose a slightly modified conjugate gradient method and for the second we proposed a method based on the generalized maximum likelihood (GML) to estimate the hyperparameters $\boldsymbol{\theta} = (\lambda, \mu)$, and the solution $\boldsymbol{x}$ by the joint maximisation:

$$(\widehat{\boldsymbol{x}},\widehat{\boldsymbol{\theta}}) = \arg \max_{\boldsymbol{x}>0,\boldsymbol{\theta}\in\Theta} \{p(\boldsymbol{x},\boldsymbol{y};\boldsymbol{\theta})\} = \arg \min_{\boldsymbol{x}>0,\boldsymbol{\theta}\in\Theta} \{J(\boldsymbol{x},\boldsymbol{\theta})\} \tag{18}$$

which is implemented iteratively,*i.e.*;

$$\widehat{\boldsymbol{x}}^{(k+1)} = \arg\min_{\boldsymbol{x}>0} \left\{ J\left(\boldsymbol{x}, \widehat{\boldsymbol{\theta}}^{(k)}\right)\right\} \tag{19}$$

$$\widehat{\boldsymbol{\theta}}^{(k+1)} = \arg\min_{\boldsymbol{\theta}\in\Theta} \left\{ J\left(\widehat{\boldsymbol{x}}^{(k)}, \boldsymbol{\theta}\right)\right\} \tag{20}$$

In this second part we present some of the imaging applications for which the proposed method has been used successfully.

3 Applications

3.1 Image reconstruction from scattered microwave field

In an imaging system using the inverse scattering, the object is illuminated by an electromagnetic wave and the scattered field is measured behind the object. The main objective of the imaging system is to obtain information about the geometric structure or any internal characteristic parameters (conductivity, permittivity, etc.) of the object. By definition, the scattered field is the difference between the fields in absence and in presence of the object. This field behaves as if it was created by an equivalent current source $\vec{J}$ which is dependent on the difference of dielectric properties (conductivity and permittivity) between the object and the background medium. $\vec{J}$ characterizes the object and is related to the scattered field $\vec{E}$ by the following expression [6, 7, 8, 9, 10, 11, 12, 13, 14] :

$$\vec{E}(\boldsymbol{r}) = -i\omega_0\mu \iiint_{(v)} \overline{\overline{G}}(\boldsymbol{r},\boldsymbol{r}')\, \vec{J}(\boldsymbol{r}')\, \mathrm{d}\boldsymbol{r}' \tag{21}$$

where $\vec{E}$ is a vectorial and complex representation of the scattered field, $\vec{J}$ is the vector which represents the equivalent current distribution, $\overline{\overline{G}}(\boldsymbol{r},\boldsymbol{r}')$ is the Green's dyadic which is given by

$$\overline{\overline{G}}(\boldsymbol{r},\boldsymbol{r}') = \left[\overline{\overline{I}} - \frac{1}{k^2}\overline{\overline{\mathrm{grad}}}_r \vec{\mathrm{grad}}_{r'}\right] \Phi \tag{22}$$

where Φ is Green's scalar function having the following form

$$\Phi = \frac{e^{-ik|\boldsymbol{r}-\boldsymbol{r}'|}}{4\pi \mid \boldsymbol{r}-\boldsymbol{r}' \mid} \tag{23}$$

and $\overline{\overline{I}}$ is the identity dyadic, k is the wave number. $\boldsymbol{r}(x,y,z)$ and $\boldsymbol{r}'(x',y',z')$ are respectively the observation point and the source point, v is the volume of the object, ω_0 is the pulsation of the incident wave and μ is the magnetic permeability of the medium.

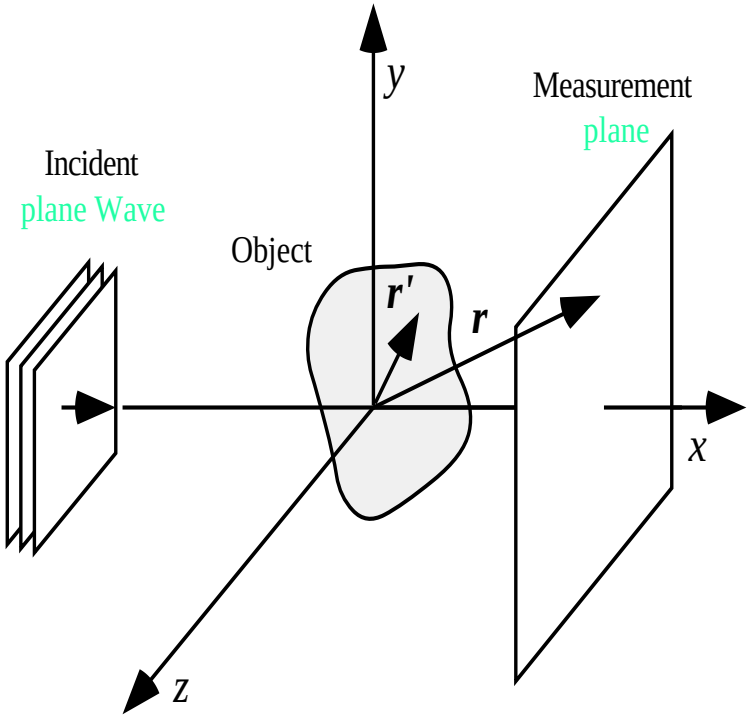

Figure 1. Geometry of the microwave tomography.

In the case of a plane-wave illumination, the vector quantities can be resumed to one component and the equation (21) becomes a scalar one. As we can see this imaging problem is a special case of the general linear inverse problem 1). So we can apply the proposed method to solve it.

Figure 2 shows a typical result of reconstruction in a two–dimensional configuration. In this figure :

a) shows the original object. By object we mean $J(x, y)$ which is assumed, in this case, to be a real quantity. $J = 0$ represents the homogeneous medium and $J \neq 0$ represents the object.

b) shows the measured scattered field $E(x, y)$ on a plane parallel to the object surface. Note that $E(x, y)$ is a complex quantity, but only its modulus is represented on the figure. We assumed that the real and imaginary parts of the measurements are independent.

c) shows the reconstructed image if a Gaussian law is chosen for the prior law, and finally,

d) shows the reconstructed image if a Gamma law is chosen for the prior law.

What can be concluded in this example is that the results are more sensible on the choice of the prior law family than on the values of its parameters. Some more details and discussions about the use of the proposed method in this application can be found in [13, 14].

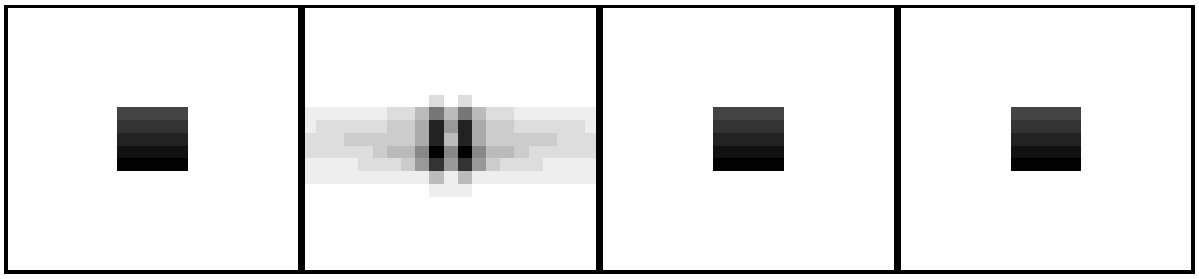

Figure 2. Image reconstruction from scattered microwave field.
a) original object $J(x, y)$
b) measured scattered field $E(x, y)$ on a plane parallel to the object surface.
c) reconstructed object from the data without noise
d) reconstructed object from the noisy data with S/N=10dB.

3.2 Image reconstruction in nondestructive evaluation using Eddy currents

In the field of non destructive control of conducting media, eddy current testing is of major importance. The object of Eddy Current Tomography is to provide a representation of the inner structure of a conductive medium in order to detect and characterize anomalies such as crack, notches, corrosion, stress. The function $f(\boldsymbol{r})$ which characterizes the object is the variation of the conductivity of the medium:

$$f(\boldsymbol{r}) = \frac{\sigma_0 - \sigma(\boldsymbol{r})}{\sigma_0}, \tag{24}$$

where σ_0 is the value of conductivity in homogeneous zones and $\sigma(\boldsymbol{r})$ is the conductivity inside the anomaly which is space-varying. $f(\boldsymbol{r})$ is a contrast function and in the homogeneous zone it fulfills $f(\boldsymbol{r}) = 0$.

The relation between the diffracted (anomalous) field $\vec{\mathcal{E}}_A$ and the object function is given by a Fredholm equation of the second type :

$$\vec{\mathcal{E}}_A(\boldsymbol{r}) = \vec{\mathcal{E}}(\boldsymbol{r}) - \vec{\mathcal{E}}_0(\boldsymbol{r}) = \int_\Omega G(\boldsymbol{r}, \boldsymbol{r}')\, f(\boldsymbol{r})\, k_2^2\, \vec{\mathcal{E}}(\boldsymbol{r}')\, \mathrm{d}\boldsymbol{r}, \tag{25}$$

where Ω is the defect volume, $k_2^2 \simeq i\mu_0\sigma_0\omega$ is the propagation constant in the homogeneous embedding, $\vec{\mathcal{E}}_0$ and $\vec{\mathcal{E}}$ are respectively the incident and the total field and $G(\boldsymbol{r}, \boldsymbol{r}')$ is a Green function. Since defects are of small size or of weak diffraction, (25) is linearized thanks to the Born approximation which assumes that inside the defect $\vec{\mathcal{E}}(\boldsymbol{r}) \simeq \vec{\mathcal{E}}_0(\boldsymbol{r})$.

The configuration we consider is presented on Figure 3. and the relevant direct problem is developed in [15, 16, 17, 4, 18]. A two-dimensional case is treated—the anomaly is invariant along the z-axis and we reconstruct its profile in the (x, y) plane. A time-harmonic normally incident electrical field $\vec{\mathcal{E}}_0$ is emitted. The measured quantity is the voltages induced into a sensing coil along a line under the conductive material and parallel to it at height $-y_0$ and this quantity is directly related to the diffracted magnetic field $\mathcal{H}_A$. Since $\vec{\mathcal{E}}_0$ is of normal incidence and $-y_0$ is fixed, the relation between the electrical and the magnetic field is given by $\frac{\mathrm{d}\mathcal{E}_A}{\mathrm{d}x} = -i\mu_0\omega\mathcal{H}_{A\,y}$, where $\mathcal{H}_{A\,y}$ is the component of $\mathcal{H}_A$ along the y-axis.

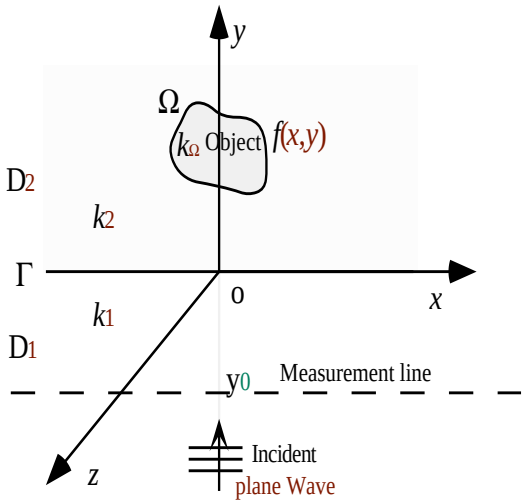

Figure 3. Geometry of the Eddy–current tomographic imaging.

The integral formulation relating the contrast function (24) and the magnetic field (which is directly proportional to the measured data) is

$$\mathcal{H}_{A\,y}(x,y_0) = -\frac{iT}{2\pi\mu_0\omega}\int_{\mathrm{R}} \underbrace{\frac{e^{-i\beta_1 y_0}}{\beta_1+\beta_2}}_{C(f,u)}\, u\, e^{iux} \underbrace{\iint_{\Omega} f(x',y')\, e^{-iux'}\, e^{i(k_2+\beta_2)y'}\,\mathrm{d}x'\,\mathrm{d}y'}_{\mathcal{F}(u)}\,\mathrm{d}u, \tag{26}$$

where $\delta = (\frac{1}{2}\omega\mu_0\sigma_0)^{-\frac{1}{2}}$ is the skin depth and decreases as the pulsation ω increase, u is the spatial frequency corresponding to the x-axis, $\beta_1 = \sqrt{k_1^2-u^2}$ and $\beta_2 = \sqrt{k_2^2-u^2}$ are the propagation factors respectively in the air and in the conductive medium with $k_1 = \sqrt{\mu_0\epsilon_0\omega^2}$—the propagation constant in the air, $k_2 = \frac{1}{\delta}(1+i)$—the propagation constant in the conductive material, and $T \simeq \frac{2k_1}{k_2}$ is the transmission coefficient on the air-metal interface. Note that β_2 and k_2 are complex, so that $\mathcal{F}(u)$ results from a Fourier transform (FT) along the x-axis and a Laplace transform (LT) along the y-axis of the object function $f(x,y)$; the LT is calculated on the algebraic curves defined by $p(u) = -i[k_2(\omega)+\beta_2(\omega,u)]$. Therefore $\mathcal{H}_{A\,y}$ is proportional to the inverse FT of a functional of $\mathcal{F}(u)$—the FLT of the image—along the algebraic curves $R \mapsto R\times C, u \mapsto (u,p)$ as defined. In order to cover the Fourier-Laplace domain better, measures are sampled for a set of electrical fields with different pulsations ω, so that in the Fourier-Laplace domain data are available along a set of parallel curves.

The image reconstruction procedure consists of determining the contrast function $f(x,y)$ from a limited set of measured data $\mathcal{H}_{A\,y}(x,y_0)$ along the measurement line. By limited set we mean limited number of pulsations ω. To solve this problem, we have two alternatives:

- Calculate first the FT of each set of data and thus covering (partially) the FLT of the contrast function $f(x,y)$, and thus transforming it to a Fourier–Laplace synthesis problem.
- Discretise the integral equation directly and try to solve the resulting linear system of equations.

In the first case more approximations can be done by neglecting entirely the attenuation ($k_2 = \frac{1}{\delta}$), or by taking it account partially [19, 4], and thus transforming the Fourier–Laplace synthesis problem to a 2–D Fourier synthesis one.

We simulated these situations and, in each of them, used the proposed Bayesian method to inverse them. In the following we show some of these results.

3.3 Method neglecting entirely the attenuation

In this case, starting by the relation 26 and neglecting entirely the attenuation, *i.e.*; $k_2 = \frac{1}{\delta}$, one can see that, the 1–D FT of the measured data for each temporal pulsation ω gives us the information about the 2–D FT of the contrast function $f(x, y)$ on a semi-circle [19, 4]. So the inverse problem to consider is, knowing the values of the 2–D FT of a function on a finite set of these semi-circles reconstruct that function. We simulated this situation by first creating a contrast function, then calculating its FT on ten semi-circles (assuming ten frequencies), and, then applied different reconstruction methods to these data to compare their performances. Figure 4 shows a typical results obtained by either some classical methods or by the proposed method.

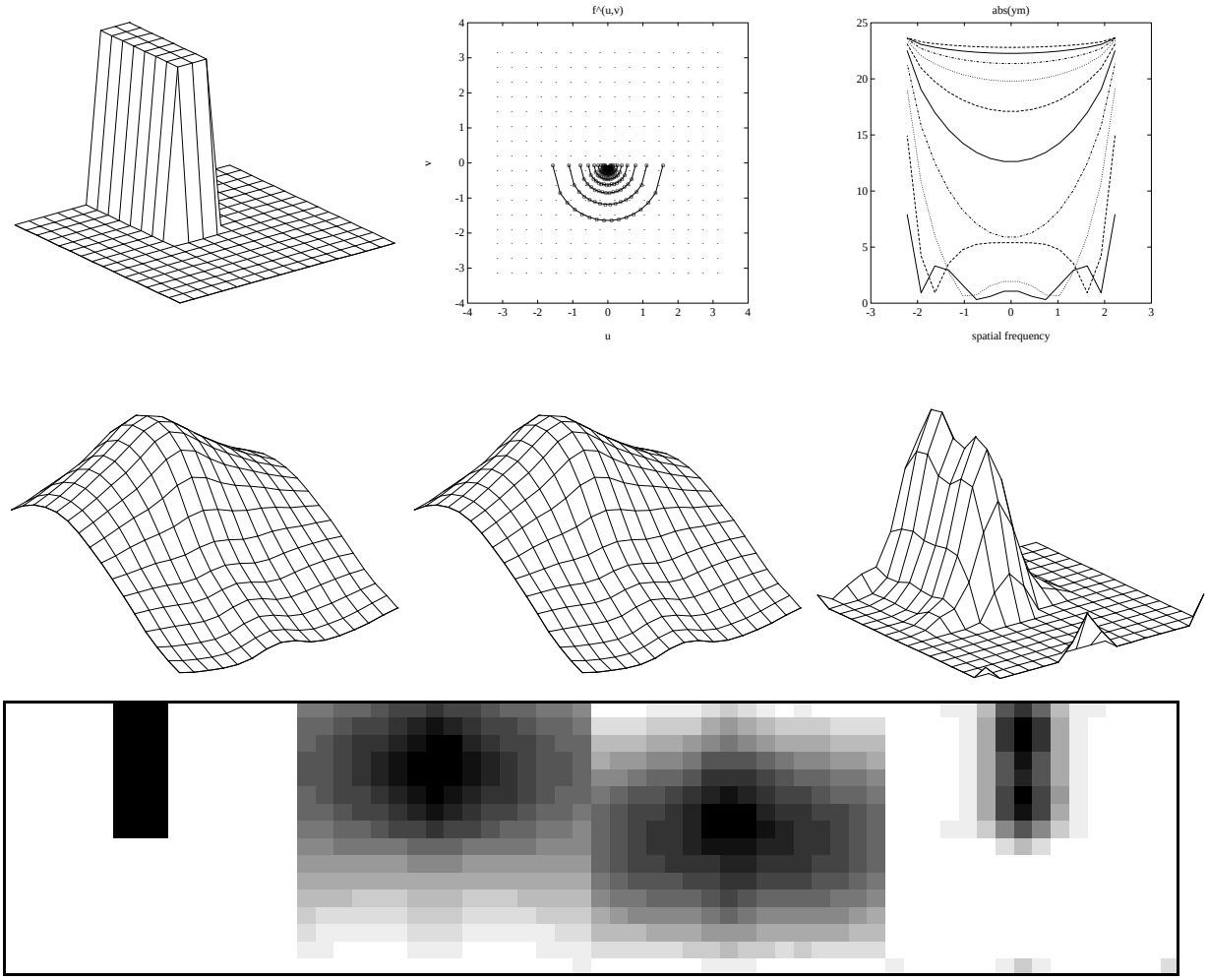

Figure 4. Eddy current tomographic image reconstruction.
(case where attenuation is entirely neglected)
a) Original contrast function $f(x, y)$,
b) Position of the data points in the Fourier domain (u, v),
c) Data values in the Fourier domain $\widehat{f}(u, v)$,
d) Reconstruction by direct FT inversion,
e) Reconstruction by a quadratic regularisation method,
f) Reconstruction by the proposed Bayesian method.
In the last line, the images a, d, e and f are presented in the form of the gray-scale images.

3.4 Method neglecting partially the attenuation

In this case also, starting by the relation 26 and replacing $k_2 + \beta_2$ by its real part, one can see that, the 1–D FT of the measured data for each temporal pulsation ω gives us the information about the 2–D FT of the contrast function $f(x, y)$ on a finite set of algebraic contours which are no more the semi-circles [19, 4]. So the inverse problem in this case also is, knowing the values of the 2–D FT of a function on a finite set of these algebraic contours reconstruct that function. Figure 5 shows a typical results obtained by the methods described in the last section.

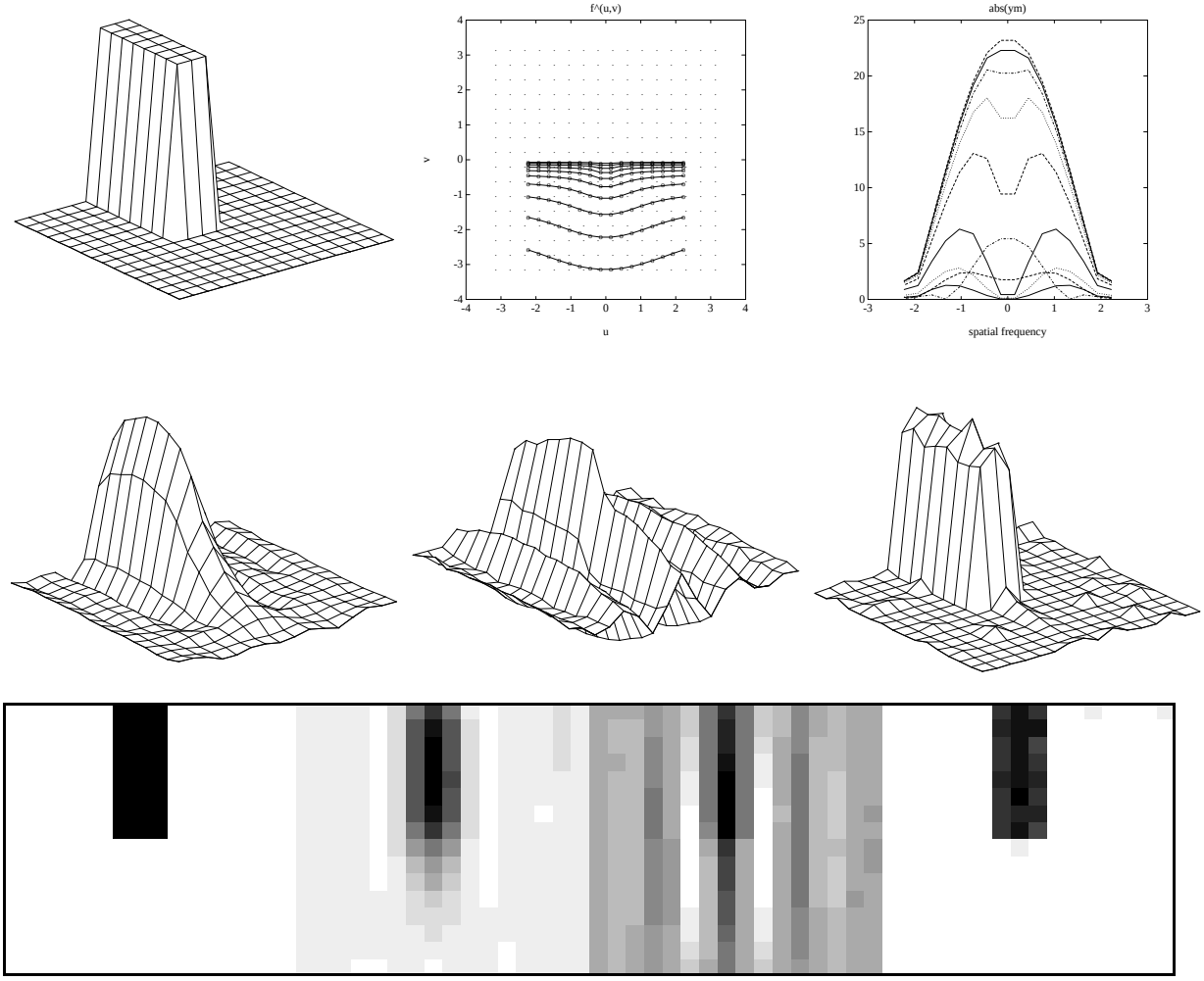

Figure 5. Eddy current tomographic image reconstruction.
(case where attenuation is partially taken into account)
a) Original contrast function $f(x, y)$,
b) Position of the data points in the Fourier domain (u, v),
c) Data values in the Fourier domain $\widehat{f}(u, v)$,
d) Reconstruction by direct FT inversion,
e) Reconstruction by a quadratic regularisation method,
f) Reconstruction by the proposed Bayesian method.
In the last line, the images a, d, e anf f are presented in the form of the gray-scale images.

3.5 Direct method taking account entirely for the attenuation

In this case the integral equation 26 is discretised directly and the resulting linear system of equations is considered and solved by the proposed method. Figure 6 shows a typical results obtained by the proposed method.

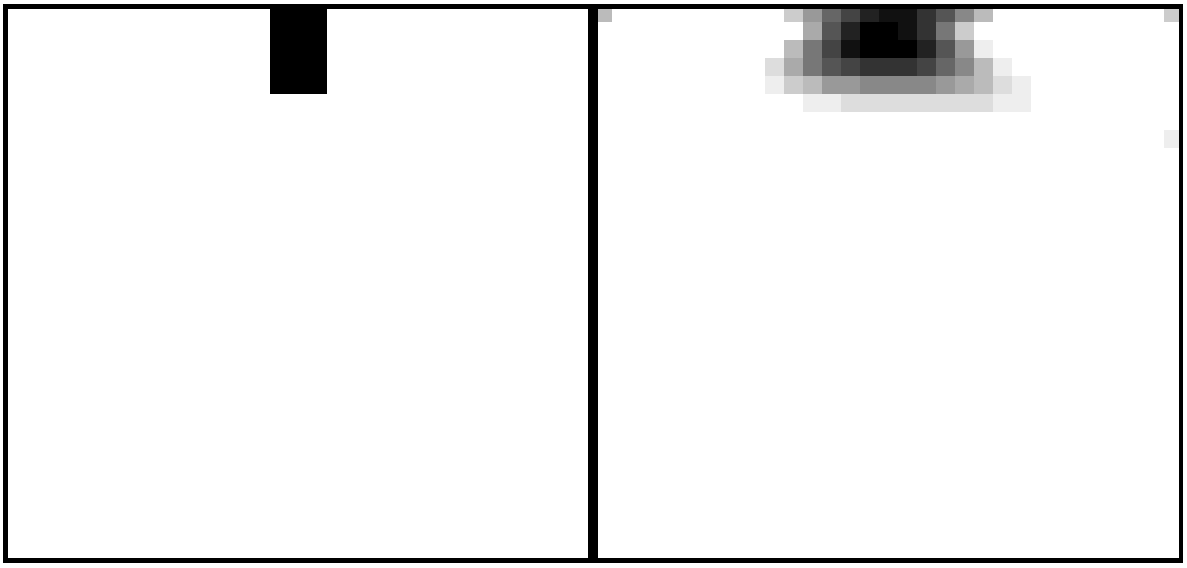

Figure 6. Eddy current tomographic image reconstruction.
(case where attenuation is totally taken into account)
a) Original contrast function $f(x, y)$,
b) Reconstruction result with the proposed method

4 Conclusions

In this paper we proposed a method based on the maximum *a posteriori* (MAP) Bayesian approach to solve the linear inverse problems (integral equations) which arise in various signal and image restoration and reconstruction problems. We used the ME principle and a scale invariance property to solve the major difficulty of the Bayesian approach which is the determination of the direct probability laws (prior law of the image and the noise). We then considered a case where we assumed to know only the noise variance and some global constraints on the image, and applied the proposed approach. The resulting Bayesian MAP estimation procedure needs an optimization algorithm. The main foundations and properties of the proposed method was discussed in the first part of this paper. In this second part we showed some original imaging applications on which the proposed method has been used successfully.

References

[1] A. Mohammad-Djafari and G. Demoment, "Maximum entropy fourier synthesis with application to diffraction tomography," *Applied Optics*, vol. 26, no. 10, pp. 1745–1754, 1987.

[2] A. Mohammad-Djafari and G. Demoment, "Tomographie de diffraction and synthèse de fourier à maximum d'entropie," *Revue Phys. Appl.*, vol. 22, pp. 153–167, 1987.

[3] A. Mohammad-Djafari and G. Demoment, "Maximum entropy reconstruction in x ray and diffraction tomography," *IEEE Transactions on Medical Imaging*, vol. 7, no. 4, pp. 345–354, 1988.

[4] M. Nikolova and A. Mohammad-Djafari, "Maximum entropy image reconstruction in eddy current tomography," in *Maximum Entropy and Bayesian Methods, Proc. of the 12th Int. MaxEnt Workshops* (A. Mohammad-Djafari and G. Demoment, eds.), (Dordrecht, The Netherlands), pp. 253–264, The 12th Int. MaxEnt Workshops, Paris, France, Kluwer Academic Publishers, 1992.

[5] A. Nikolova, M.and Mohammad-Djafari and J. Idier, "Inversion of large-supported ill-conditioned linear operators using a markov model with line process," in *Proceedings of IEEE ICASSP*, vol. V, pp. 357–360, 1994.

[6] A. Ishimaru, *Wave propagation and scattering in random media.* New York: Academic Press, 1978.

[7] A. Devaney and M. Oristaglio, "Inversion procedure for inverse scattering within the distorted-wave born approximation," *Physical Review Letters*, vol. 51, pp. 237–240, 1983.

[8] G. Beylkin and M. Oristaglio, "Distorted wave born and distorted wave rytov approximations," *Optics Communications*, vol. 53, pp. 213–216, 1985.

[9] D. Hill, "Electromagnetic scattering by buried objects of low contrast," *IEEE Trans. Geoscience and Remote Sensing*, vol. 26, pp. 195–203, 1988.

[10] M. David and M. Kirdy, "Recent improvements to the application of the volume integral method of eddy current modeling," *Journal of nondestructive Evaluation*, vol. 8, pp. 45–52, 1989.

[11] Y. Wang and W. Chew, "An iterative solution of the two-dimensional electromagnetic inverse scattering problem," *Int. Journal of Imaging Systems and Technology*, vol. 1, pp. 100–108, 1989.

[12] G. Chew and Y. Wang, "Reconstruction of two-dimensional permittivity distribution using the distorted born iterative method," *IEEE Transactions on Medical Imaging*, vol. 9, pp. 218–225, 1990.

[13] M. Nguyen and A. Mohammad-Djafari, "Bayesian maximum entropy image reconstruction from the microwave scattered field data," in *Maximum Entropy and Bayesian Methods* (A. Mohammad-Djafari and G. Demoment, eds.), (Dordrecht, The Netherlands), pp. 253–264, The 12th Int. MaxEnt Workshops, Paris, France, Kluwer Academic Publishers, 1992.

[14] M. Nguyen and A. Mohammad-Djafari, "Bayesian approach with the maximum entropy principle in image reconstruction from microwave scattered field data," *IEEE Transactions on Medical Imaging*, vol. 13, pp. 254–261, June 1994.

[15] R. Zorgati, *Imagerie par courants de Foucault.Application au contrôle non destructif.* PhD thesis, Universitde Paris VII, Thèse de Doctorat, Paris, 1990.

[16] R. Zorgati, B. Duchene, D. Lesselier, and F. Pons, "Eddy current testing of anomalies in conductive materials, part i: Qualitative imaging via diffraction tomography techniques," *IEEE Transactions on Magnetics*, vol. 27, pp. 4416–4437, 1991.

[17] D. Prémel, *Imagerie des milieux conducteurs par courants de Foucault.* PhD thesis, Université de Paris-Sud, Thèse de doctorat en Sciences, Orsay, Dec. 1992.

[18] D. Prémel and A. Mohammad-Djafari, "Eddy current tomography in cylindrical geometry," *To appear in: IEEE Trans. on Magnetics*, May 1995.

[19] M. Nikolova, "Tomography de diffraction par courants de foucault pour le contrôle non destructif des milieux conducteurs," rapport de stage de dea, Université de Paris-Sud, 1991.